ADVANCED MATERIALS
www.advmat.de

Materials Views
www.MaterialsViews.com

Autonomic Restoration of Electrical Conductivity

Benjamin J. Blaiszik, Sharlotte L. B. Kramer, Martha E. Grady, David A. McIlroy, Jeffrey S. Moore, Nancy R. Sottos, and Scott R. White**

Thermomechanical failure of conductive pathways in highly integrated circuits results in loss of function that is often impossible to repair and remains a long-standing problem hindering advanced electronic packaging.[1–3] Prior approaches to restoration of conductivity rely on external intervention in the form of heating[4] or manual delivery of relatively low conductivity materials.[5,6] Here, we demonstrate autonomic healing of an electrical circuit with nearly full recovery of conductance (ca. 99%) less than one millisecond after damage. The rapid restorative mechanism relies on the triggered release and transport of microencapsulated eutectic gallium–indium (Ga–In) liquid metal into the broken conductive pathway. For a relatively small volume fraction of microcapsules that are patterned on gold (Au) lines, all of the damaged circuits heal with high efficiency. This autonomic healing system shows the potential for more sustainable electronic devices with increased fault-tolerance, improved circuit reliability, and extended service life.

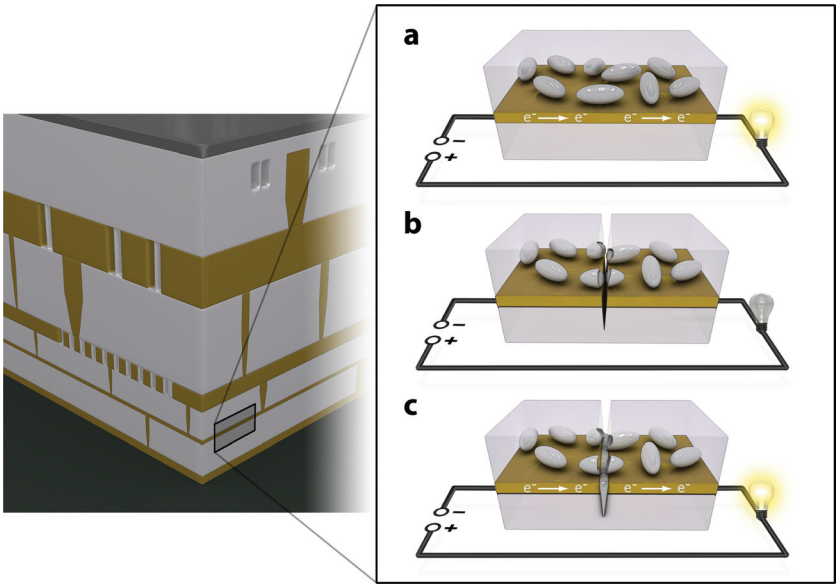

Figure 1. Autonomic conductivity restoration concept in a multilayer microelectronic device. a) The self-healing circuit consists of microencapsulated liquid metal dispersed in a dielectric material and deposited on a conductive line. b) Crack damage breaks the conductive pathway, interrupting electron transport and simultaneously rupturing the capsules. c) The liquid metal flows from the capsules to the area of damage, restoring a conductive pathway.

The demand for smaller electronics with increased performance and functionality drives the development of complex, high-density integrated circuits and robust packaging that operate in adverse environments. Scaling of planar integrated circuits, to satisfy Moore's Law,[7] has resulted in devices with large numbers of thin, patterned conductive films (typically Cu or Al) separated by dielectric layers and interconnected through multiple levels of conductive vias. Recent advances in 3D integration[1,8,9] and flexible circuitry[10] have further enhanced performance and functionality. As integration and packaging of microelectronic devices become more complex, the multiscale and dissimilar nature of the constituent materials leads to reliability issues that impair electrical performance of the entire system. Loss of conductivity in electronic circuits occurs through interconnect fracture,[2,3] conductive pathway delamination,[11,12] thin film cracking,[13,14] and other mechanisms.[15–17] These circuit failures degrade functionality, requiring costly replacement of the entire component. Self-healing circuits that rely on hardware redundancy or delay-insensitive asynchronous logic have been proposed to address reliability concerns with only modest success.[18–20]

Here, we introduce a materials-based approach, shown schematically in **Figure 1**, to autonomously restore conductivity in a broken circuit. Healing is accomplished by the release and transport of a microencapsulated conductive material to the site of damage. Eutectic Ga-In alloy is chosen as the healing agent due to its low melting point, ca. 16 °C, its relatively high conductivity of 3.40×10^4 S•cm^{-1},[21] and its previously demonstrated

Dr. B. J. Blaiszik, Dr. S. L. B. Kramer, Dr. D. A. McIlroy, Prof. N. R. Sottos
Department of Materials Science and Engineering
Beckman Institute for Advanced Science and Technology
University of Illinois at Urbana-Champaign
1304 W. Green St. Urbana, IL 61801, USA
E-mail: n-sottos@illinois.edu
M. E. Grady
Department of Mechanical Science and Engineering
University of Illinois at Urbana-Champaign
1206 W. Green St. Urbana, IL 61801, USA
Prof. J. S. Moore
Department of Chemistry
Beckman Institute for Advanced Science and Technology
University of Illinois at Urbana-Champaign
505 S. Mathews St. Urbana, IL 61801, USA
Prof. S. R. White
Department of Aerospace Engineering
Beckman Institute for Advanced Science and Technology
University of Illinois at Urbana-Champaign
104 S. Wright St. Urbana, IL 61801, USA
E-mail: swhite@illinois.edu

DOI: 10.1002/adma.201102888

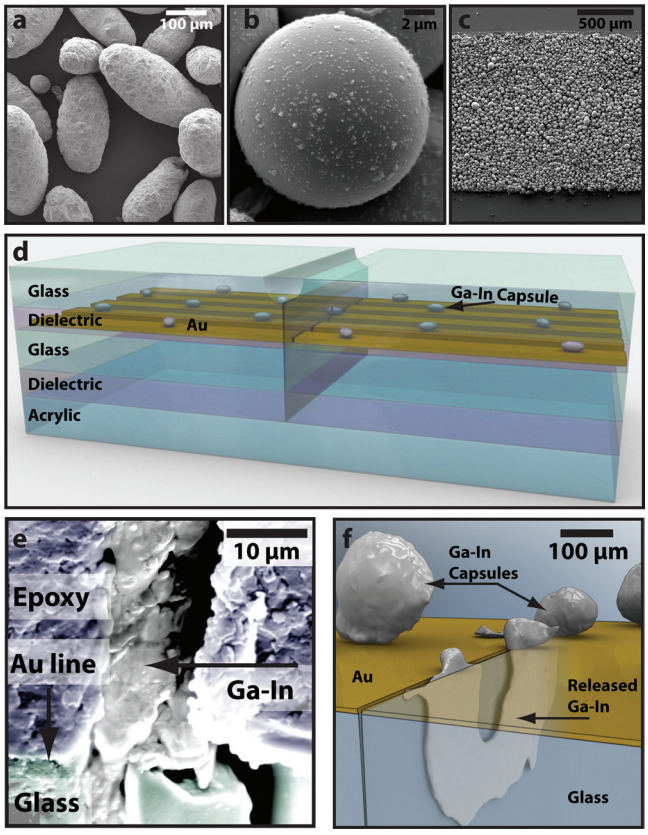

Figure 2. Self-healing circuit components, multilayer test specimen, and evidence of triggered release. SEM images of: a) ca. 200 µm diameter Ga-In-filled UF microcapsules; b) ca. 10 µm diameter Ga-In UF microcapsule; and c) ca. 10 µm diameter capsules patterned on an Au line. d) Schematic image of a multilayer test specimen consisting of a glass substrate with a 100 nm thick Au line pattern, epoxy dielectric with dispersed Ga-In microcapsules, notched glass top layer, and acrylic bottom layer. Crack damage initiates at the notch root and propagates through the specimen before arresting and debonding at the acrylic interface. e) Cross-sectional SEM image showing the location of the damaged area and subsequent liquid metal release (false color). f) Micro-CT data, with schematic superimposed, showing microcapsules and liquid metal that has been released into the crack plane of a healed specimen.

ability to form conformal electrodes.[22] Liquid Ga–In is encapsulated in a polymeric urea-formaldehyde (UF) shell wall.[23] Representative scanning electron microscopy (SEM) images of ellipsoidal Ga–In filled capsules with major-axis length ca. 200 µm are presented in **Figure 2**a. With a core of liquid Ga–In, the shell wall of the microcapsules is likely a combination of the polymer and a metal oxide passivation layer that forms rapidly when Ga–In is exposed to oxygen.[24] The capsule size is controlled by varying the processing conditions (see the Supporting Information, Figure S1). Through the use of sonication,[25] capsules as small as 3 µm in diameter are produced. Interestingly, as capsule diameter is reduced, the capsule shape becomes more spherical (Figure 2b).

To demonstrate the self-healing potential of microencapsulated liquid metals, we examine the performance in a model multilayer device before and after mechanical damage (Figure 2d). A conductive circuit is formed by patterning Au lines on a rigid glass substrate. An epoxy dielectric layer is deposited on top of the conductive circuit. Larger diameter (ca. 200 µm) Ga–In microcapsules are embedded in the dielectric layer, or smaller diameter (ca. 10 µm) capsules are patterned directly onto the Au lines (Figure 2c).

The device is bonded to a notched glass top layer and a ductile acrylic bottom layer and loaded in four-point bending to provide controlled and repeatable circuit failure. At a critical bending load, a crack initiates at the notch root and propagates through the dielectric layer and conductive Au line, finally arresting at the bonded acrylic interface. The embedded microcapsules are ruptured during crack propagation releasing liquid metal into the damaged circuit. Specimens are imaged using electron microscopy and micro-computed tomography (micro-CT), revealing the localized release and transport of Ga–In alloy into the crack plane (Figure 2e,f).

The circuit is monitored throughout the four-point bend test using a Wheatstone Bridge with the specimen as one bridge arm (Supporting Information, Figure S2). We track the performance of the circuit by measuring the normalized bridge voltage, $V_{norm} = (V_h - V_\infty)/(V_o - V_\infty)$, where V_o is the bridge voltage before damage, V_∞ is the bridge voltage measured for a fully broken circuit, and V_h is the instantaneous bridge voltage of the circuit. The value of V_{norm} ranges from zero for a specimen with no electrical conductance to one for a fully conductive specimen. The efficiency of conductivity restoration, η_c, is defined for each specimen as V_{norm} after fracture.

Representative mechanical and electrical responses for both self-healing and control specimens are shown in **Figure 3**. The bending load increases linearly and then precipitously drops when crack propagation occurs. The load plateaus as the crack arrests at the acrylic layer, and a delamination crack propagates along the acrylic/epoxy interface. When fracture occurs, V_{norm} simultaneously drops to zero, correlating to a broken circuit (i.e., V_h approaches V_∞).

In a self-healing specimen with Ga–In microcapsules (Figure 3a), V_{norm} rapidly recovers to over 99% of the undamaged value ($\eta_c > 99\%$). In great contrast, a control specimen containing no microcapsules (neat epoxy dielectric layer) shows no recovery even after unloading (Figure 3b). Additional control specimens were fabricated with a dielectric layer containing either solid Ga microcapsules or solid glass beads, and no healing was observed. In self-healing specimens, we also monitored resistance between adjacent Au lines, and no short circuits occurred. For a subset of healed samples, conductivity was periodically monitored for up to four months following the healing event with no loss of conductivity observed.

To investigate the time scale for recovery of conductivity, we monitored the normalized bridge voltage of a subset of samples at a sampling rate of 2.5 MHz. For the self-healing specimen containing Ga-In capsules (Figure 3a), the normalized bridge voltage quickly returns to 0.99 after 20 µs. For the subset of samples monitored, the average healing time was 160 µs. Restoration of conductivity occurs approximately 7 orders of magnitude faster than the time required for recovery of fracture toughness in prior microcapsule-based self-healing.[26]

The effect of Ga–In capsule concentration on healing is summarized in Figure 3c (see also the Supporting Information, Table S1). For specimens containing ca. 200 µm diameter

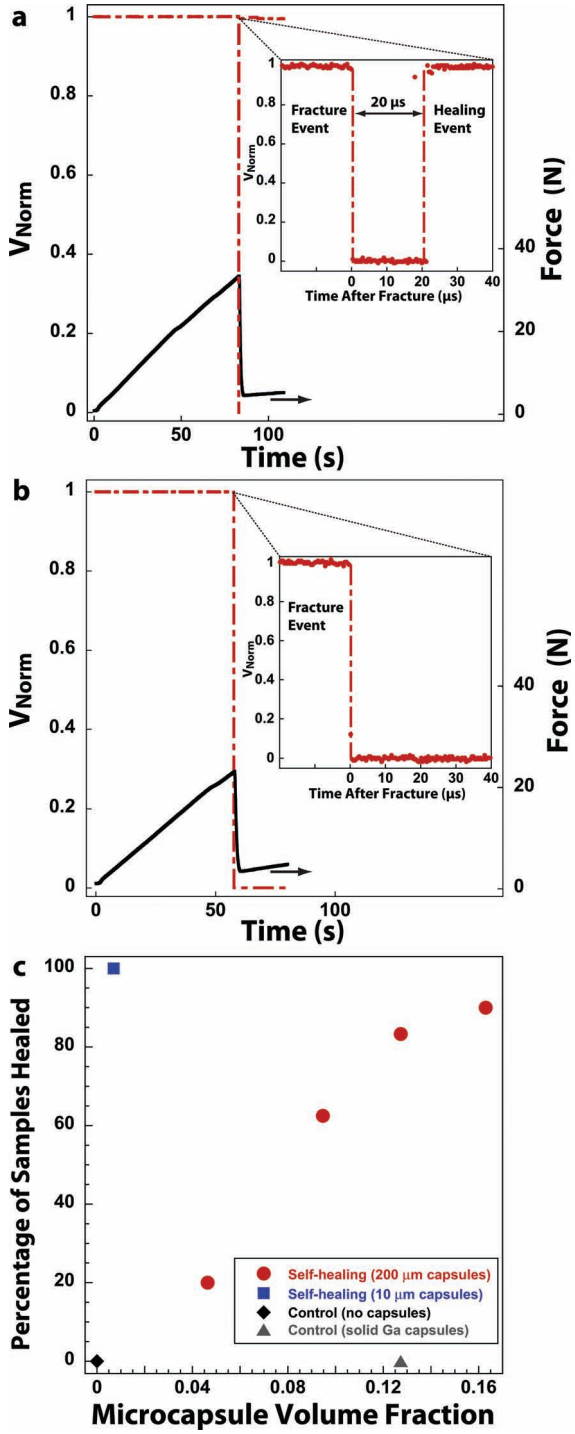

Figure 3. Autonomic restoration of conductivity. Evolution of the normalized bridge voltage (red dash) and force (black) during four-point bend tests of a self-healing specimen (a) and a control specimen (b). Zoomed plots of the normalized bridge voltage (V_{norm}) at the time of fracture for a representative self-healing specimen (inset in (a)) show the time scale associated with recovery of conductivity and for a representative control specimen (inset in (b)) show no recovery. c) The percentage of samples where healing was observed increases as the volume fraction of 200 μm diameter capsules increases. All samples with 10 μm diameter capsules patterned on the Au line fully healed. Restoration of conductivity was not observed for any control specimen (neat epoxy, glass bead inclusions, solid Ga capsules).

Ga-In capsules, the percentage of specimens that heal is proportional to the volume fraction of capsules included in the dielectric epoxy layer. At the maximum volume fraction tested (0.16), 90% (9/10) of the samples healed. For the specimens that heal, nearly full recovery of conductance is achieved (η_c = 99%), independent of microcapsule volume fraction. Remarkably, for specimens with a volume fraction of only 0.007 patterned ca. 10 μm diameter capsules (Figure 2c), 100% (7/7) of the samples healed with high efficiency (η_c = 98%). Hence, restoration is achieved with low concentrations of smaller capsules specifically targeted to the location of damage. We conclude that increasing capsule volume fraction or decreasing capsule size increases the probability that the propagating crack will intersect and rupture a capsule. When the crack intersects a capsule, the released liquid metal forms a conductive pathway and healing occurs with high efficiency. Optimal recovery of conductance may require a variety of capsule sizes depending on the size scales of the circuit damage.

We have demonstrated autonomic restoration of electrical conductivity in a mechanically damaged circuit. Self-healing circuits will lead to increased longevity and device reliability in adverse mechanical environments, enabling new applications in microelectronics, advanced batteries, and electrical systems. Beyond self-repairing devices, we envision the concepts described here could enable microelectronics that generate new circuits along stress-activated pathways, allowing for adaptive circuit architecture and improved circuit redundancy.

Experimental Section

Encapsulation of Liquid Metal: Liquid Ga–In eutectic alloy (Ga obtained from GalliumSource, LLC and In obtained from Strem Chemicals) is encapsulated via an in situ reaction of urea and formaldehyde following an encapsulation method from prior work[23] (see also the Supporting Information: Microencapsulation Details).

Lithography Technique: A lift-off lithography technique is used to pattern Au on glass substrates in a class 1000 cleanroom, using AZ5214E photoresist (AZ Electronic Materials). The substrates are coated with a thin layer of Cr (10 nm) followed by Au (100 nm) using electron-beam deposition, and then submerged in acetone to lift off the remaining photoresist and unwanted Au/Cr, leaving only the desired Au/Cr pattern adhered to the substrates (see also the Supporting Information: Lithography Method).

Au/Cr Film Pattern: Each Au/Cr film pattern is comprised of five electrically isolated Au/Cr lines that span the length of the glass slide. The lines are spaced 1.0 mm apart and have a line width of 1.5 mm. The center Au/Cr line is monitored via the Wheatstone Bridge voltage, and the other lines are used to test for internal short circuits after mechanical testing. The crack separation at the Au/Cr line after unloading is approximately 5–10 μm.

Sample Geometry: Four-point bend specimens have dimensions of 12.0 mm wide × 75.0 mm long × 4.0 mm thick. The notched glass and epoxy/microcapsule layers are 60 mm long to accommodate electrical contacts on either end of the Au lines. Specimen layer thickness dimensions are 1.5 mm acrylic (McMaster-Carr), 250 μm epoxy dielectric (Epon 828-DETA from Miller-Stephenson), 1.0 mm glass, 10 nm Cr, 100 nm Au, 250 μm epoxy dielectric and liquid metal capsules, and 1.0 mm of glass treated with (3-trimethoxysilylpropyl)-diethylenetriamine (Gelest, Inc.) with a central rounded notch ca. 500 μm deep (see also the Supporting Information: Specimen Preparation).

Four-Point Bend Fracture Testing: A custom four-point bend loading frame includes a base with adjustable pin spacing (nominally 55 mm),

top fixture with 16 mm pin spacing, load cell (Futek LSB200–45 N max capacity), amplifier (Omega DP25B-S-A), linear actuator (Physik Instrumente M-230.25 S) for displacement of the top fixture, and LabVIEW 2009 for actuator control and load data acquisition.

Wheatstone Bridge Circuit: The four-point bend specimen acts as one resistor in an unbalanced constant voltage Wheatstone Bridge circuit. The voltage source is a BK Precision DC Power Supply (model 1710). The bridge voltage and voltage source are monitored through a LabVIEW DAQ and/or a digital oscilloscope (LeCroy LC584A) (see also the Supporting Information: Unbalanced Wheatstone Bridge).

Supporting Information

Supporting Information is available from the Wiley Online Library or from the author.

Acknowledgements

This material is based upon work supported as part of the Center for Electrical Energy Storage - Tailored Interfaces, an Energy Frontier Research Center funded by the U.S. Department of Energy, Office of Science, Office of Basic Energy Sciences under Award Number (919 DOE ANL 9F-31921 NS). We acknowledge the support of the Semiconductor Research Corporation Education Alliance Master's Scholarship Program for Martha E. Grady's funding. We would like to thank Susan A. Odom and Amanda R. Jones for helpful discussions related to this work, the University of Illinois Beckman Institute Imaging Technology Group for help with Micro-CT and SEM imaging, and Ryan Durdle, Alex Jerez, and Jeremy Miller of the Beckman Institute VMIL for their schematic artwork contributions. Sample preparation was carried out in part in the Frederick Seitz Materials Research Central Facilities, University of Illinois, which is partially supported by the U.S. Department of Energy.

Received: July 27, 2011
Revised: October 30, 2011
Published online: December 20, 2011

[1] J. Knickerbocker, P. Andry, B. Dang, R. Horton, M. Interrante, C. Patel, R. Polastre, K. Sakuma, R. Sirdeshmukh, E. Sprogis, S. Sri-Jayantha, A. Stephens, A. Topol, C. Tsang, B. Webb, S. Wright, *IBM J. Res. Dev.* **2008**, *52*, 553.
[2] T. Mattila, J. Kivilahti, *J. Electron. Mater.* **2006**, *35*, 250.
[3] Y. Chan, D. Yang, *Prog. Mater. Sci.* **2010**, *55*, 428.
[4] K. A. Williams, A. J. Boydston, C. W. Bielawski, *J. R. Soc. Interface* **2007**, *4*, 359.
[5] M. M. Caruso, S. R. Schelkopf, A. C. Jackson, A. M. Landry, P. V. Braun, J. S. Moore, *J. Mater. Chem.* **2009**, *19*, 6093.
[6] S. Odom, M. Caruso, A. Finke, A. Prokup, J. Ritchey, J. Leonard, S. White, N. Sottos, J. Moore, *Adv. Funct. Mater.* **2010**, *20*, 1721.
[7] G. E. Moore, *Electronics* **1965**, *38*, 114.
[8] S. Sri-Jayantha, G. McVicker, K. Bernstein, J. Knickerbocker, *IBM J. Res. Dev.* **2008**, *52*, 623.
[9] T. S. Cale, J. Lu, R. J. Gutmann, *Chem. Eng. Commun.* **2008**, *195*, 847.
[10] Q. Cao, H. Kim, N. Pimparkar, J. Kulkarni, C. Wang, M. Shim, K. Roy, M. Alam, J. Rogers, *Nature* **2008**, *454*, 495.
[11] R. H. Dauskardt, M. Lane, Q. Ma, N. Krishna, *Eng. Fract. Mech.* **1998**, *61*, 141.
[12] V. K. Khanna, *J. Phys. D Appl. Phys.* **2011**, *44*, 034004.
[13] J. Ambrico, E. Jones, M. Begley, *Int. J. Solid. Struct.* **2002**, *39*, 1443.
[14] Z. Xia, J. Hutchinson, *J. Mech. Phys. Solids* **2000**, *48*, 1107.
[15] A. Gallo, R. Munamarty, *IEEE T. Reliab.* **1995**, *44*, 362.
[16] Q. Guo, C. Whitman, L. Keer, Y. Chung, *J. Appl. Phys.* **1991**, *69*, 7572.
[17] C. Chen, H. Tong, K. Tu, *Annu. Rev. Mater. Res.* **2010**, *40*, 531.
[18] I. Koren, Z. Koren, *Proc. IEEE* **1998**, *86*, 1819.
[19] T. Tseng, Y. Huang, J. Li, *IEEE T. Comput. Aid. D.* **2010**, *29*, 1628.
[20] B. Rahbaran, A. Steininger, *IEEE T. Depend. Secure* **2009**, *6*, 282.
[21] D. Zrnic, D. Swatik, *J. Less-Common Met.* **1969**, *18*, 67.
[22] R. Chiechi, E. Weiss, M. Dickey, G. Whitesides, *Angew. Chem. Int. Ed.* **2008**, *47*, 142.
[23] E. Brown, M. Kessler, N. Sottos, S. White, *J. Microencapsul.* **2003**, *20*, 719.
[24] M. Dickey, R. Chiechi, R. Larsen, E. Weiss, D. Weitz, G. Whitesides, *Adv. Funct. Mater.* **2008**, *18*, 1097.
[25] B. Blaiszik, N. Sottos, S. White, *Comp. Sci. Tech.* **2008**, *68*, 978.
[26] S. White, N. Sottos, P. Geubelle, J. Moore, M. Kessler, S. Sriram, E. Brown, S. Viswanathan, *Nature* **2001**, *409*, 794.